

# FABRICATION OF NANO-STRUCTURED CADMIUM ZINC TELLURIDE THIN FILMS

**Dr. MONISHA CHAKRABORTY**

Assistant Professor, School of Bio-Science & Engineering, Jadavpur University, 188, Raja S. C. Mallik Road, Kolkata-700032, India.

## ABSTRACT

In this work, proper methods are adopted to fabricate large area, nano-structured  $Cd_{1-x}Zn_xTe$  thin films of 100nm thickness for 'x' varying from 0.0567 to 0.2210. The fabricated films are subjected to optical and structural characterization studies. Properties of fabricated films are found to vary with 'x'. Particle size obtained from X-Ray Diffraction (XRD) analysis is found to match well with Field Emision Scanning Electron Microscope (FESEM) result. The results confirm the nano-structure of the fabricated films.

**Keywords -**  $Cd_{1-x}Zn_xTe$  Thin films, Field Emision Scanning Electron Microscope (FESEM), Nano-structure, Optical characterization, Structural characterization, X-Ray Diffraction (XRD) analysis.

## I. INTRODUCTION

II-VI compound semiconductors have the optical band gap in the visible region and these materials are used worldwide for optoelectronic devices [1-5]. CdTe is one such compound in this group and its physical properties are continually examined during the recent past. Its fascinating properties make the material suitable for many potential applications. CdTe is a potential material for solar cell. CdTe alloyed with zinc, makes  $Cd_{1-x}Zn_xTe$ , which is a tunable, wide, direct band-gap ternary semiconductor and it is one of the few room temperature solid-state gamma radiation detector materials commercially available [6-7]. This material can provide gamma ray spectra suitable for isotope identification. In the recent years, major attention has been given to the investigation of electrical, optical and structural properties of  $Cd_{1-x}Zn_xTe$  thin films in order to improve the performance of the device and also for finding new applications. A comprehensive review of the material properties of  $Cd_{1-x}Zn_xTe$  with varying zinc content is reported in [8, 16]. Some studies on the structural and optical properties of II-VI compound semiconductors are proposed previously and these are reported in [9-18].

The properties of  $Cd_{1-x}Zn_xTe$  film varies with the concentration of 'x'. So, determination of 'x' in CZT matrix is an important aspect. The range of 'x' in  $Cd_{1-x}Zn_xTe$  lies preferably within  $0.05 \leq x \leq 0.95$  [16, 19]. Band gap of an alloy is a function of the concentration, 'x' of its constituents. The method to determine the variation of band gap energy with varying concentrations of zinc ions, has been reported in [20]. In the present paper, the variation of band gap of nano-structured  $Cd_{1-x}Zn_xTe$  100 nm thin films with 'x' has been studied. Photoluminescence (PL) is a suitable technique to determine the crystalline quality and

presence of impurities in the material. In the present work, PL spectra of nano-structured  $Cd_{1-x}Zn_xTe$  100 nm thin films are studied. In this work, fabricated nano-structured  $Cd_{1-x}Zn_xTe$  100 nm thin films are subjected to X-Ray Diffraction (XRD) studies. Particle size and strain are obtained from XRD analysis and particle size is also confirmed by Field Emision Scanning Electron Microscope (FESEM) analysis.

Owing to extensive research and industrial work conducted by teams of solid-state physicists, engineers and medical physicists, CdTe/CZT detectors are now widely used. CdTe/CZT-based surgery probes have large impact on patient management in surgical oncology. Excellent large-field of view modules have already been realized as reported in [21]. The performance of a CZT dual Positron Emission Tomography (PET), dedicated for breast cancer, is studied by a group of researchers and these are reported in [22]. Studies in [23] report on dedicated emission mammotomography with CZT imaging detector. Works are published in [24] where researchers fabricated metal-semiconductor-metal planar  $Cd_{1-x}Zn_xTe$  detectors from large  $Cd_{1-x}Zn_xTe$  single crystals. The study in [25] reports on the detailed investigation of the optical properties of CdZnTe crystals grown by vertical Bridgman method.

In this work, proper methods are adopted to fabricate nano-structured  $Cd_{1-x}Zn_xTe$  thin films of 100 nm thickness and these are discussed in section II of this paper. The mathematical calculation for obtaining 'x' is discussed in section III of this paper. The optical characterization results of nano-structured  $Cd_{1-x}Zn_xTe$  100 nm thin films are discussed in section IV of this paper. PL spectra of these fabricated  $Cd_{1-x}Zn_xTe$  100nm thin films are studied and these results are discussed in section V of this paper. The structural characterization results of these fabricated films are discussed in section VI of this paper. Particle size and strain for  $Cd_{1-x}Zn_xTe$  100 nm thin films are obtained from XRD analysis and these are discussed in section VII of this paper. Particle size is also obtained from FESEM study and this has been discussed in section VIII of this paper. The significance of the results of this work is discussed in section IX of this paper. The work is concluded in section X of this paper.

## II. MATERIALS AND METHODS

In this work, physical deposition method is adopted to fabricate six large-area, nano-structured thin films of  $Cd_{1-x}Zn_xTe$  of 100 nm thickness. Surface cleaning of the substrate has predominant effect on the growth of the film on it. Thus prior to deposition, glass substrates are carefully cleaned. Commercially available glass slides of dimensions 23 mm x 37 mm x 1 mm are dipped in chromic acid for 2

hours. These are washed with detergent and finally ultrasonically cleaned with acetone before use.

In order to design the six different compositions of nano-structured Cd<sub>1-x</sub>Zn<sub>x</sub>Te 100 nm thin films, six different % ratio of the stack layer of ZnTe/CdTe is chosen and these are 20:80, 30:70, 40:60, 50:50, 60:40 and 70:30. For these six ratios of the stack layer of ZnTe/CdTe, six different values of 'x' are obtained. The mathematical detail is discussed with a sample calculation in section III of this paper.

For the film fabrication, 500W RF Sputtering unit has been used. ZnTe and CdTe targets are placed in the target holders of the RF sputtering unit. Plain glass substrates are kept at the bottom of the target holder and temperature to the order of 100°C is maintained on the substrates. Argon gas is injected from outside and pressure of the order of 10<sup>-2</sup> Torr has been maintained. At this pressure, the RF unit is energized and a power of 500W with a frequency of 13.56 MHz is applied between the target and the substrate. On application of this RF power the target gets energized and vapour of the target material produced deposits on the substrate. At the substrate temperature the film gets crystallized and the thickness is dependent on the sputtering time. Both CdTe and ZnTe targets are sputtered sequentially and a stack layer of ZnTe/CdTe is thus obtained. The stack layer is then annealed in vacuum (10<sup>-5</sup> Torr) for an hour at 300°C. Both Cadmium and Zinc tried to inter-diffuse among each other to get into a stabilized state. Applications of thermal energy initiate both cadmium and zinc inter-diffusion. However, the stoichiometric ratio of cadmium and zinc is not equal and as a result the film is formed in the form of Cd<sub>1-x</sub>Zn<sub>x</sub>Te. The value of 'x' decides whether the film is CdTe or ZnTe. Thickness and deposition time for CdTe and ZnTe layers for each composition of nano-structured Cd<sub>1-x</sub>Zn<sub>x</sub>Te thin films of 100 nm thickness are tabulated in Table 1. The schematic of fabricated film for optical and structural characterization studies is shown in Fig. 1.

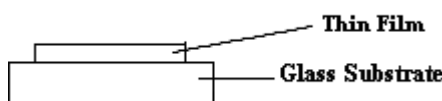


Fig. 1 Schematic of fabricated film for optical and structural characterization

### III. SAMPLE CALCULATION OF 'X'

In this section, the mathematics to determine 'x' in nano-structured Cd<sub>1-x</sub>Zn<sub>x</sub>Te thin film of 100 nm thickness is discussed with a sample calculation. For this purpose, one out of the six samples is considered and this is a 100 nm stack of CZT comprised of ZnTe film deposited on CdTe film. Percentage thickness ratio of ZnTe : CdTe layer is 60:40 and this can be expressed as given in Eq. (1.1).

$$\frac{\% \text{ZnTe}}{\% \text{CdTe}} = \frac{60}{40} = \frac{n_{\text{ZnTe}}}{n_{\text{CdTe}}} = \frac{m_{\text{ZnTe}}}{M_{\text{CdTe}}} \quad (1.1)$$

where,

m<sub>ZnTe</sub> and m<sub>CdTe</sub> are the masses of ZnTe and CdTe layers respectively to attain the % ratio ZnTe : CdTe as 60:40.

M<sub>ZnTe</sub> and M<sub>CdTe</sub> are the molar masses of ZnTe and CdTe respectively and these values are M<sub>ZnTe</sub> = 193 gms/mol and M<sub>CdTe</sub>=240 gms/mol. On putting these values, Eq. (1.1) becomes,

$$1.5 = \frac{\rho_{\text{ZnTe}} \cdot T_{\text{ZnTe}} \cdot A.240}{\rho_{\text{CdTe}} \cdot T_{\text{CdTe}} \cdot A.193} \quad (1.2)$$

where,

'A' is the cross-sectional area of the substrate. ρ<sub>ZnTe</sub> and ρ<sub>CdTe</sub> are the density of ZnTe and CdTe layers respectively and these values are ρ<sub>ZnTe</sub> = 6.34 gms/cc and ρ<sub>CdTe</sub>=5.85 gms/cc. T<sub>ZnTe</sub> and T<sub>CdTe</sub> are the values of thickness of ZnTe and CdTe layers respectively. On putting these values, Eq. (1.2) becomes,

$$\frac{T_{\text{ZnTe}}}{T_{\text{CdTe}}} = 1.113022477 \quad (1.3)$$

$$T_{\text{ZnTe}} + T_{\text{CdTe}} = 100 \text{ nm} \quad (1.4)$$

Solutions of Eq. (1.3) and Eq. (1.4) give the values of the thickness of CdTe and ZnTe layers and these are,

$$T_{\text{CdTe}} = 47.33 \text{ nm} \text{ and } T_{\text{ZnTe}} = 52.67 \text{ nm.} \quad (1.5 \text{ a})$$

Deposition rates for CdTe and ZnTe targets are 78 nm/min and 45 nm/min respectively.  $(1.5 \text{ b})$

From Eq. (1.5 a) and Eq. (1.5 b) the deposition times for CdTe and ZnTe layers for this sample are obtained and these values are t<sub>CdTe</sub> = 36 sec and t<sub>ZnTe</sub> = 1min 10 sec respectively.  $(1.5 \text{ c})$

So, mass of ZnTe layer, m<sub>ZnTe</sub> = 333.96.A.10<sup>-7</sup> gms and mass of CdTe layer, m<sub>CdTe</sub> = 276.86.A.10<sup>-7</sup> gms.

Molar mass of Zinc, M<sub>Zn</sub> = 65.38 gms/mol.

So, 113.93.A.10<sup>-7</sup> gms of zinc is present in 333.96.A.10<sup>-7</sup> gms of ZnTe.

∴ Fraction of zinc in this CZT matrix

$$= \frac{113.93 \cdot A \cdot 10^{-7}}{(276.86 + 333.96) \cdot A \cdot 10^{-7}} = 0.1865 \quad (1.6)$$

Similarly, for other % ratios of ZnTe : CdTe layers considered in this study, the values of 'x' are calculated and the results are tabulated in Table 1.

### IV. OPTICAL CHARACTERIZATION AND RESULTS

The six samples of nano-structured Cd<sub>1-x</sub>Zn<sub>x</sub>Te thin films of 100 nm thickness are subjected to optical characterization studies. Transmission and reflection spectra of these samples are recorded using PerkinElmer Lambda 35 spectrophotometer and the plots of normalized values of (αhv)<sup>2</sup> vs. hv are obtained.

A sample plot showing the variation of (αhv)<sup>2</sup> vs. hv obtained for nano-structured Cd<sub>1-x</sub>Zn<sub>x</sub>Te thin film of 100 nm thickness for the composition at 'x' = 0.1865 is shown in Fig. 2. From such curve, energy band gap of the fabricated film can be evaluated<sup>[8, 16, 18]</sup>. The band-gap of this sample is found to be 1.9980 eV. For other values of 'x', the energy band gaps are similarly obtained. Fig. 3 shows the variation of band gap with 'x'. It is observed in Fig. 3 that band gap of the fabricated film is a function of 'x'.

Table 1 Thickness and Deposition Times of ZnTe and CdTe layers in 100 nm CZT Films

S.No.	(%ZnTe):(%CdTe)	Thickness of ZnTe layer T <sub>ZnTe</sub> (nm)	Thickness of CdTe layer T <sub>CdTe</sub> (nm)	Deposition time for CdTe layer t <sub>CdTe</sub>	Deposition time for ZnTe layer t <sub>ZnTe</sub>	Fraction of Zinc in CZT matrix, 'x'
1	20:80	15.65	84.35	1 min 5 sec	21 sec	0.0567
2	30:70	24.13	75.87	58 sec	32 sec	0.0870
3	40:60	33.10	66.90	51 sec	44 sec	0.1182
4	50:50	42.60	57.40	44 sec	57 sec	0.1510
5	60:40	52.67	47.33	36 sec	1 min 10 sec	0.1865
6	70:30	63.39	36.61	28 sec	1 min 25 sec	0.2210

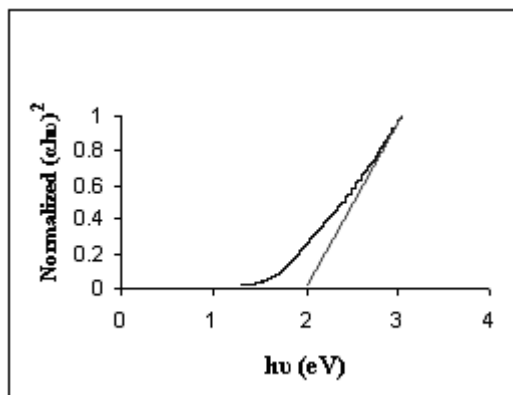


Fig. 2 Variation of  $(\alpha \cdot h \cdot v)^2$  vs.  $h \cdot v$  of nano-structured  $\text{Cd}_{1-x}\text{Zn}_x\text{Te}$  100 nm thin film at ' $x$ ' = 0.1865

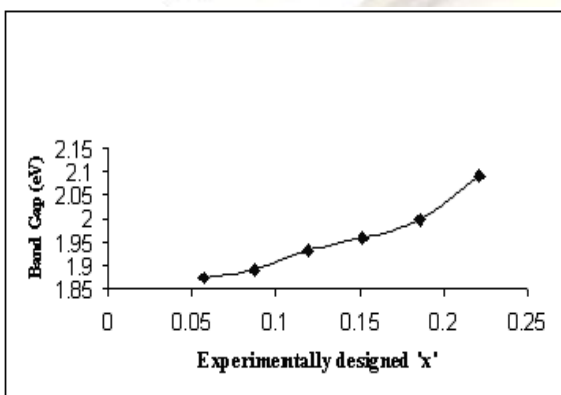


Fig. 3 Variation of band gap energy with ' $x$ '

## V. PHOTOLUMINESCENCE RESULTS

Photoluminescence (PL) spectra for nano-structured  $\text{Cd}_{1-x}\text{Zn}_x\text{Te}$  100 nm thin films, deposited on glass substrate, are obtained for different ' $x$ ', with photo-excitations at 450 nm. PL studies are done using PerkinElmer LS 55 luminescence spectrometer. The typical plot of room temperature PL spectra of nano-structured  $\text{Cd}_{1-x}\text{Zn}_x\text{Te}$  100 nm thin film for ' $x$ ' = 0.1865 is shown in Fig. 4 as sample result.

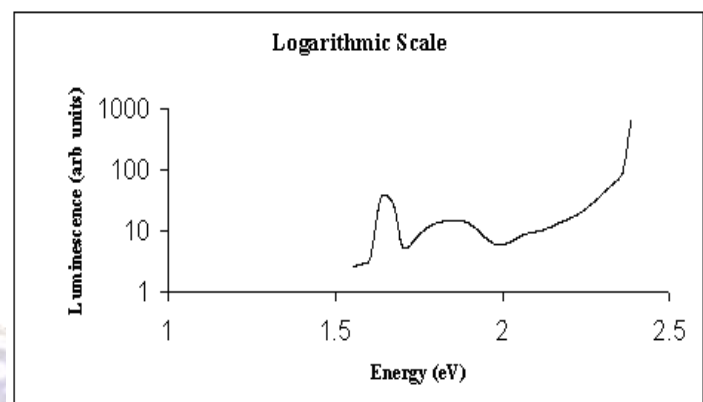


Fig. 4 Room Temperature PL spectra of nano-structured thin film of  $\text{Cd}_{1-x}\text{Zn}_x\text{Te}$  of 100 nm thickness at ' $x$ ' = 0.1865

Similarly, for other values of ' $x$ ' of nano-structured  $\text{Cd}_{1-x}\text{Zn}_x\text{Te}$  100 nm thin films, plots of room temperature PL spectra are obtained.

## VI. STRUCTURAL CHARACTERIZATION AND RESULTS

X-Ray Diffraction (XRD) spectra of the fabricated films are recorded on Rigaku Miniflex (Japan) powder diffractometer using  $\text{Cu K}\alpha$  radiation ( $1.5406 \text{ \AA}$ ). The scanning angle range,  $2\theta$  of the diffractometer, is from  $20^\circ$  to  $70^\circ$ . XRD spectra of nano-structured  $\text{Cd}_{1-x}\text{Zn}_x\text{Te}$  100 nm thin film at ' $x$ ' = 0.1865 is shown in Fig. 5 as sample result. At constant temperature, crystal lattice constant of an alloy bears a linear relationship with the concentrations of the constituent elements<sup>[26]</sup>. For a simple cubic lattice, the lattice constant bears a relation with  $d$ -value where ' $d$ ' is the spacing between adjacent parallel planes<sup>[27]</sup>. So, this implies that the  $2\theta$  values of the peaks of nano-structured  $\text{Cd}_{1-x}\text{Zn}_x\text{Te}$  100 nm thin films at ' $x$ ' = 0.1865, as shown in Fig. 5 will lie in between the  $2\theta$  values of the peaks of the corresponding planes of  $\text{CdTe}$  and  $\text{ZnTe}$  cubic crystals. On the basis of this idea and standard JCPDS files, CZT peaks in the XRD spectra of nano-structured  $\text{Cd}_{1-x}\text{Zn}_x\text{Te}$  100 nm thin films at ' $x$ ' = 0.1865 are identified and the details of these results are tabulated in Table 2(a). Peaks other than CZT are also identified in the XRD spectra of nano-structured  $\text{Cd}_{1-x}\text{Zn}_x\text{Te}$  100 nm thin films at ' $x$ ' = 0.1865 and the details of these results are tabulated in Table 2(b).

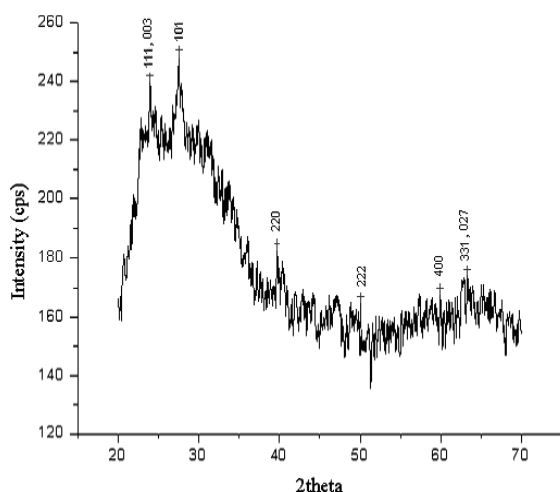


Fig. 5 XRD spectra of nano-structured  $\text{Cd}_{1-x}\text{Zn}_x\text{Te}$  thin film at ' $x$ ' = 0.1865

Similarly, for other values of ' $x$ ' of nano-structured  $\text{Cd}_{1-x}\text{Zn}_x\text{Te}$  100 nm thin films, XRD spectra are obtained and their respective results have shown a good agreement with standard JCPDS files. CZT planes in nano-structured  $\text{Cd}_{1-x}\text{Zn}_x\text{Te}$  100 nm thin films are thus identified and these are tabulated in Table 3. The details of the identified CZT planes include the values of inter-planar spacing i.e.  $d$ -values, FWHM, peak no. and  $I/I_0$  and these are tabulated in Table 3 for nano-structured  $\text{Cd}_{1-x}\text{Zn}_x\text{Te}$  100 nm thin films at various ' $x$ '. The absence of CZT planes are marked as blank in Table 3.

## VII. DETERMINATION OF STRAIN AND PARTICLE SIZE

The FWHM ( $\beta$ ) can be expressed as a linear combination of the contributions from the strain ( $\varepsilon$ ) and particle size ( $L$ ) as given by Eq. (1.7) [26, 28].

$$\frac{\beta \cos \theta}{\lambda} = \frac{1}{L} + \frac{\varepsilon \sin \theta}{\lambda} \quad (1.7)$$

Plots showing the variation of  $\frac{\sin \theta}{\lambda}$  vs

$\frac{\beta \cos \theta}{\lambda}$  obtained from nano-structured  $\text{Cd}_{1-x}\text{Zn}_x\text{Te}$

100 nm thin film for the composition at ' $x$ ' = 0.1865 is shown in Fig. 6 as sample result.

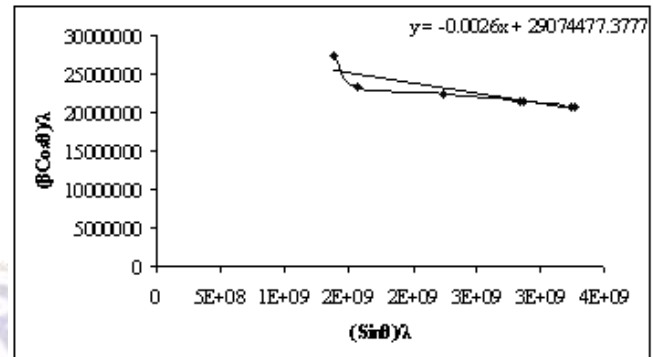


Fig. 6 Variation of  $(\sin \theta)/\lambda$  vs  $(\beta \cos \theta)/\lambda$  of nano-structured thin film of  $\text{Cd}_{1-x}\text{Zn}_x\text{Te}$  of 100 nm thickness at ' $x$ ' = 0.1865

Similarly, for other values of ' $x$ ', such plots showing the variation of  $(\sin \theta)/\lambda$  vs  $(\beta \cos \theta)/\lambda$  for nano-structured  $\text{Cd}_{1-x}\text{Zn}_x\text{Te}$  100 nm thin films are obtained. Particle size is obtained from the intercept and strain is obtained from the slope of these plots. Particle size and strain are found to be 34.39 nm and -0.0026 respectively for nano-structured  $\text{Cd}_{1-x}\text{Zn}_x\text{Te}$  100 nm thin film at ' $x$ ' = 0.1865. Similarly, for other values of ' $x$ ', particle sizes and strains are obtained. Variation of strain with particle size for all the compositions of nano-structured  $\text{Cd}_{1-x}\text{Zn}_x\text{Te}$  100 nm thin films is shown in Fig. 7.

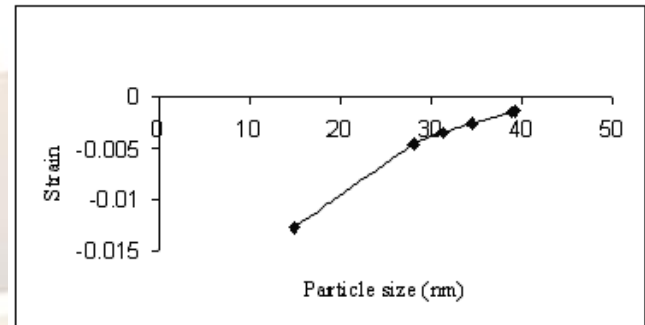


Fig. 7 Variation of strain with particle size for nano-structured thin films of  $\text{Cd}_{1-x}\text{Zn}_x\text{Te}$  of 100 nm thickness

Table 2(a) Details of CZT peaks in nano-structured  $\text{Cd}_{1-x}\text{Zn}_x\text{Te}$  100 nm thin film at ' $x$ ' = 0.1865

S. No.	Peak No.	2theta (deg)	I/I <sub>0</sub>	Planes	JCPDS Card No.
1	3	23.93	89	111	CdTe-150770-ZnTe-800022
2	3	23.93	89	003	CZT- 471296
3	10	39.68	62	220	CdTe-150770-ZnTe-800022
4	10	39.68	62	220	CZT- 471296
5	13	49.82	48	222	CdTe-752083-ZnTe-800002
6	16	59.93	58	400	CdTe-752083-ZnTe-800022
7	21	62.93	47	331	CdTe-150770-ZnTe-752085
8	21	62.93	47	027	CZT- 471296

Table 2(b) Details of other peak in nano-structured  $\text{Cd}_{1-x}\text{Zn}_x\text{Te}$  100 nm thin film at ' $x$ ' = 0.1865

S. No.	Peak No.	2theta (deg)	I/I <sub>0</sub>	Planes	JCPDS Card no
1	6	27.47	100	101	Te-850555

Table 3 Details of identified CZT planes in nano-structured  $\text{Cd}_{1-x}\text{Zn}_x\text{Te}$  100nm thin films

Fraction of Zinc (x)	111	003	200	220	311	400	420	331	027	021	222
0.0567	3.7200 0.282 3 100	3.7200 0.282 3 100	3.1596 0.212 6 40	2.2259 0.212 13 57	1.8941 0.247 16 41	1.5715 0.212 19 45	1.4043 0.212 21 43				
0.0870	3.7062 0.282 3 81		1.3648 0.212 21 65		1.8975 0.212 14 63		1.3899 0.212 20 62				
0.1182	3.6926 0.212 2 20	3.6926 0.212 2 20	3.1335 0.212 7 9				1.4225 0.282 26 30	1.4744 0.247 24 17	1.4744 0.247 24 17		
0.1510			3.1174 0.247 5 38		1.9363 0.212 13 29	1.5457 0.212 17 35		1.4839 0.212 18 33	1.4839 0.212 18 33		
0.1865	3.7154 0.212 3 89	3.7154 0.212 3 89		2.2695 0.176 10 62		1.5421 0.212 16 58		1.4756 0.212 21 47	1.4756 0.212 21 47		1.8287 0.176 13 48
0.2210	3.6701 0.212 4 20			2.2323 0.388 13 21	1.9294 0.247 17 14			1.4769 0.282 21 15		3.6701 0.212 4 20	1.8350 0.212 18 18

### VIII. FESEM ANALYSIS

Field Emision Scanning Electron Microscope (FESEM) is used to study the fine structure surface morphology of the fabricated film. From FESEM analysis, size and shape of particles are obtained. FESEM of  $\text{Cd}_{1-x}\text{Zn}_x\text{Te}$  thin film of 100 nm thickness at ' $x$ ' = 0.1865 is obtained using Jeol 6700F Field Emision Scanning Electron Microscope and this is shown in Fig. 8 at a magnification scale of 1,00000 as sample result.

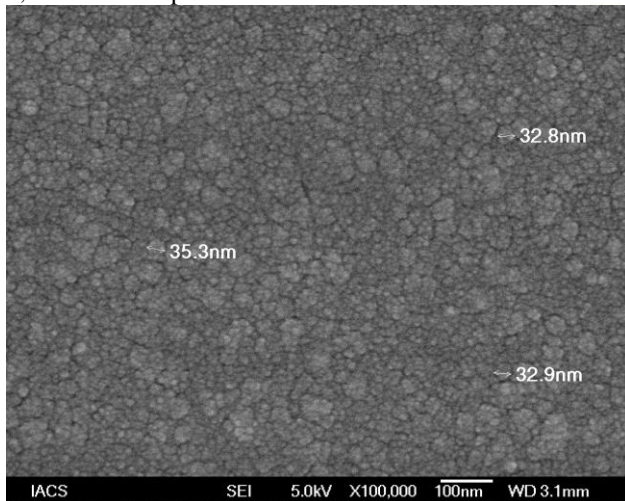


Fig. 8 FESEM photograph of nano-structured  $\text{Cd}_{1-x}\text{Zn}_x\text{Te}$  100 nm thin film at ' $x$ ' = 0.1865 at 1,00000 magnification

FESEM photograph as shown in Fig. 8 indicates the amorphous nature of the deposited film. Also, the average particle size for  $\text{Cd}_{1-x}\text{Zn}_x\text{Te}$  thin film of 100 nm thickness at ' $x$ ' = 0.1865 is about 33.67 nm as shown in Fig. 8.

### IX. DISCUSSIONS

Optical results reveal that band gap of fabricated nano-structured  $\text{Cd}_{1-x}\text{Zn}_x\text{Te}$  100 nm thin films is a function of ' $x$ '. There is increase in band gap with increase in ' $x$ ' as observed in Fig. 3. From the PL spectra, as shown in Fig. 4, it is observed that the sharpness of the peaks of nano-structured  $\text{Cd}_{1-x}\text{Zn}_x\text{Te}$  100 nm thin film at ' $x$ ' = 0.1865 is much less. Similar observations are obtained for other values of ' $x$ '. This may be due to the predominance of nano-structured dimensional effect [17]. In the X-ray Diffraction (XRD) patterns of nano-structured  $\text{Cd}_{1-x}\text{Zn}_x\text{Te}$  100 nm thin films, for ' $x$ ' varying from 0.0567 to 0.2210, the peaks for CZT along with other peaks are identified. Results obtained from XRD analysis have shown a good agreement with standard JCPDS files. The peak heights and widths for identified planes are found to vary with ' $x$ '. Some

peaks are found to lie between those for  $\text{CdTe}$  and  $\text{ZnTe}$  as discussed in section VI of this paper. Results obtained from XRD analysis indicate that ' $x$ ' is the parameter, in controlling the structure of the films. From the XRD spectra, as shown in Fig. 5, it is observed that the sharpness of the identified peaks is much less. Similar observations are obtained for other values of ' $x$ '. This may be due to the predominance of nano-structured dimensional effect [18]. Particle size and strain are obtained for nano-structured thin films of  $\text{Cd}_{1-x}\text{Zn}_x\text{Te}$  of 100 nm thickness and these are discussed in section VII of this paper. It has been observed from Fig. 7 that with the decrease in particle size, compressive strain increases. From FESEM analysis, the average particle size for  $\text{Cd}_{1-x}\text{Zn}_x\text{Te}$  thin film of 100 nm thickness at ' $x$ ' = 0.1865 is found to be about 33.67 nm as shown in Fig. 8. The particle size for the same film, obtained from XRD analysis is found to be 34.39 nm. So, there is a close matching in the values of particle size obtained from XRD analysis and FESEM analysis as shown in Fig. 8.

### X. CONCLUSION

This study infers that optical and structural properties of fabricated nano-structured  $\text{Cd}_{1-x}\text{Zn}_x\text{Te}$  100 nm thin films are functions of ' $x$ '. Decrease in particle size results in the increase in compressive strain. The value of particle size obtained from XRD analysis and FESEM analysis is found to be in close agreement to each other and these results confirm the nano-structure of the fabricated  $\text{Cd}_{1-x}\text{Zn}_x\text{Te}$  100 nm thin films.

### ACKNOWLEDGEMENTS

Author is thankful to all the members of Advanced Materials and Solar Photovoltaic Division, School of Energy Studies, Jadavpur University, Kolkata, India for their help and cooperation.

### REFERENCES

- [1] R. K. Willardson, A. C. Beer, *Semiconductors and Semimetals*, 13, Academic, New York, 1978.
- [2] J. P. Faurie, J. Reno and M. Boukerche, *J. Crystal Growth*, 72, 1985, 111.
- [3] T. E. Schlesinger, R. B. James, *Semiconductors and Semimetals*, 43, Academic, San Diego, 1995.
- [4] R. Dornhaus, G. Nimitz, G. Höhler and E. A. Nickisch, *Springer*, 1983, 119.
- [5] Z. Q. Shi, C. M. Stahle and P. Shu, *Proc. SPIE*, 90, 1998, 3553.

- [6] J. Gaines, R. Drenten, K. Haberbern, P. Menz and J. Petruzzelo, *Appl. Phys. Lett.*, 62, 1993, 2462.
- [7] J. Pal, PhD Thesis, Jadavpur University, Kolkata, India, 2005.
- [8] T. E. Schlesinger, J. E. Toney, H. Yoon, E. Y. Lee, B. A. Brunett, L. Franks and R. B. James, *Material Science and Engineering*, 32, 2001, 103.
- [9] D. Patidar, K. S. Rathore, N. S. Saxena, K. Sharma, T. P. Sharma, *Chalcogenide Letters*, 5, 2008, 21.
- [10] B. Samanta, S. L. Sharma and A. K. Chaudhuri, *Vacuum*, 46, 1995, 739.
- [11] M. Li and J. C. Li, *Materials Letters*, 60, 2006, 2526.
- [12] S. Herrera, C. M. Ramos, R. Patino, J. L. Pena, W. Cauich, A. I. Oliva, *Brazilian Journal of Physics*, 36, 2006.
- [13] A. Nag, S. Sapra, S. Sen Gupta, A. Prakash, A. Ghangrekar, N. Periasamy, D. Sarma, *Bull. Mater. Sci.*, 31, 2008, 561.
- [14] C. N. R. Rao, G. U. Kulkarni, P. J. Thomas, P. P. Edwards, *Chem. Eur. J* 8, 2002, 29.
- [15] J. L. Reno. and E. D. Jones, *Phys. Rev.* 45, 1992, 1440.
- [16] M. Chakraborty, *International Journal of Engineering Science and Technology*, 3(5), 2011, 3798-3806.
- [17] M. Chakraborty, *International Journal of Engineering Science and Technology*, 3(10), 2011, 7402-7407.
- [18] M. Chakraborty, *International Journal of Engineering Research and Applications*, 1(4), 2011, 2096-2104
- [19] Weblink:  
<http://www.freepatentsonline.com/5528495>.
- [20] G. P. Joshi, N. S. Saxena, R. Mangal, A. Mishra, and T. P. Sharma, *Bull. Mater. Sci.*, 26, 2003, 387.
- [21] Y. Eisen, I. Mardor, A. Shor, et al. *IEEE Trans. Nucl. Sci.*, 49, 2002, 172.
- [22] H. Peng, P. D. Olcott, G. Pratz, A. M. K. Foudray, G. Chinn, C. S. Levin, *IEEE Nuclear Science Symposium Conference Record*, 2007.
- [23] C. N. Brzymialkiewicz, M. P. Tornai, R. L. McKinley and J. E. Bowsher, *IEEE Transactions on Medical Imaging*, 24, 2005, 7.
- [24] A. Burger, M. Groza, Y. Cui, D. Hillman, E. Brewer, A. Bilikiss, G. W. Wright, L. Li, F. Lu and R. B. James, *Journal of Electronic Material*, 32, 2003, 7.
- [25] L. Guoqiang and J. Wanqi, *Materials Science Forum*, 475, 2005, 1841.
- [26] A. R. Denton, N. W. Ashcroft, *Physical Review A (Atomic, Molecular, and Optical Physics)*, 43, 1991, 3161.
- [27] C. Kittel, C, *Introduction to Solid State Physics*, John Wiley & Sons, 7<sup>th</sup> ed, 1996.
- [28] S. B. Quadri, E. F. Skelton, D. Hsu, A. D. Dinsmore, J. Yang, H. F. Gray and B. R. Ratna, *Phys. Rev., B* 60, 1999, 9191.